Construction and Evaluation of modern EVs drive system

Hossein Mousazadeh[*1], *Alireza Keyhani*[1], *Arzhang Javadi*[2], *Hossein Mobli*[1], *Karen Abrinia*[3] and *Ahmad Sharifi*[2]
[1.] *Department of Agricultural Machinery Engineering, University of Tehran, Karaj, Iran.*
[2.] *Agr. Eng. Res. Ins. (AERI), Karaj, Iran.*
[3.] *College of Engineering, University of Tehran, Iran.*

Corresponding author: Tel/Fax: 0098-0261-2808138. e-mail: hmousazade@gmail.com*

Abstract- *Ever –increasing in climate changing forces to shift to friendly and clean energy alternatives such as renewable energies that their output is usually electricity. Noticeable part of these air pollutions is from tailpipe of internal combustion engines. EVs could be parity by conventional Internal Combustion Engine Vehicles (ICEV) in near future. They are simplest way to replace fossil fuel powered vehicles. EVs are relatively cheap, have little environmental impact and are a technology which is available here and now. Using an electronic control board and two power boards, a high power EV drive system was designed and constructed (designed for the vehicles up to 100 kW). The controller uses power IGBT module and microcontroller technology to simultaneously control two DC series motors. The driver controls direction of motion and causes differential speeds of motors relative to steering rod and acceleration pedal position. Driver simulation in MATLAB proved that the required conditions of the problem were satisfied by PID controller; and the optimum values for the control parameters K_p, K_i and K_d were found to be 320, 350 and 40, respectively. The result of simulation for these motors indicated that for start up a high torque is available.*

Keywords: *Duty cycle; Motor driver; PID control; Simulink; Unit step; steady-state error.*

Nomenclature

a	*The number of current paths.*
b	*Damping ratio of mechanical system, [Nms]*
c	*Coefficient between flux and armature current*
E_A	*internal generated voltage, [V]*
I_A	*Armature current, [A]*
k	*Electromotive force constant, [Nm/Amp]*
$K.c$	*Motor constant*
L	*Electric inductance, [H]*
p	*The number of motor poles*
R	*Armature and field resistance, [ohms]*
T_{ind}	*Conducted torque, [Nm]*
V_T	*Terminal voltage, [V]*
Z	*Total number of conductors*
φ	*Stator flux*

1. Introduction

Reduction in oil and fossil fuel resources force the mankind to seek other energy resources. The consumption of fossil fuels also has environmental impacts. Electric energy from renewable resources is the most important and clean source of energy that can be converted into today's need in effective ways.

All mechanisms of EVs almost consist of electrical systems. The EV drive system also uses electric and electronic circuits to operate. Silva et al. (2007) evaluated a remote experiment for controlling a motor using a PID algorithm programmed in Lab View environment. They tested the algorithm by different proportional, integral and differential values [1]. Mrozek et al. (2000) simulated an industrial DC driver using two techniques: fuzzy control and PID control. They concluded, despite the fact that the fuzzy drive was successful, the fuzzy controller was more difficult to design compared to PID [2]. Pravadalioglu (2005) designed, constructed and evaluated a permanent magnet DC motor drive using PI type fuzzy controller. He simulated the controller by MATLAB and compared simulink and experimental results. It was noted that the designed driver showed better performance in a wide range of applications [3]. Kumar et al. (2008) designed an artificial neural controller for a closed loop speed control of DC drive, fed by a DC chopper as Pulse Width Modulation (PWM). In their algorithm the signal corresponding to DC motor error, feeds as an ANN controller input. They concluded that the designed system has less computation time than that of the conventional controller [4]. Nouri et al. (2008) proposed an adaptive control of a DC motor using neural network. They validated experimentally the performance of a recurrent neural network structure

combined with the inverse model control on a DC motor drive system and reported good performance results [5]. Thirusakthimurugan et al. (2007) designed and simulated a permanent magnet brushless DC motor drive system for speed and position controls. Their simulation results indicated that the proposed control performance is precise for up to 6–10 times that of rotor inertia changes [6]. Santana et al. (2002) simulated and constructed a speed controller for a 1 hp DC series motor. They simulated the controller voltage, current, torque as a function of each other and time. Their simulations showed that the system should not be started up with a duty cycle above 50% [7]. Massacci et al. (2006) designed and constructed an electronic device for motors control in mobile robotics applications. Their controller used the classical PID control as a implemented law, whose parameters could be changed also while working, through the serial connections, and from the wireless [8]. Al-Ayasrah et al. (2008) evaluated a two-Synchronized Motors Control System Using External FPGA Design for a variety of applications. In their proposed technique an external FPGA structural design is interfaced with the PWM Generation Unit of a dual core Digital Signal Processor (DSP) board for the use of Two-Motor Control using one DSP Processor [9]. Xepapas et al (2001) evaluated a Nonlinear Geometric Fuzzy Logic Controller for DC machines and the simulation results compared by PI controller. They concluded that the proposed controller has better performance when is compared to the conventional PI controller. Although the input of the Geometrical Fuzzy logic controller is only the error of the speed, the response is better because it takes the advantage of the derivative of the speed error [10]

The aim of this study is design, construction and assessment of a DC motor controller suitable for EVs drive system, also definition of optimum control technology to studied DC motors is the other part of this paper.

2. Materials and methods

The series DC motors have more application in vehicles, trucks and lift trucks. Two DC series motors with 80V, 160A and 10.5kW power were selected for this study. The driver system is designed and constructed in the electric Lab. of Agricultural Machinery Engineering Department of Tehran University. In this drive system an electronic control board interfaces between the power board and operator. There are two power boards; each for controlling one of the DC motors. When operator accelerates the throttle, an analogue voltage that connected to ADC bus of microcontroller increases in the range of 0 to 5V. Corresponding to the input voltage, the output duty cycle of PWM channel from micro is varied. The 5V PWM output amplified to a maximum of 12V using a buffer so is fed to the power board. Increasing the PWM of microcontroller increases the average of power voltage in head of the motors that led to high speeds (fig (1)).

Simultaneously two PWM output from the micro becomes ON and two IGBTs from power units are activated to allow the current to flow in the corresponding direction. If the motor speed changes from a predefined value due to load changes, the encoder feedbacks this signal error and the microcontroller compensates this error using desired control strategy. In series to the acceleration potentiometer a twist grips steering potentiometer that is connected by gear to the steering rod, changes the duty cycle (duty cycle is the time ratio at which the switch is 'on') and creates the differential needed between two motors when steering. The motors are synchronized for different modes (for straight motion and turning modes).

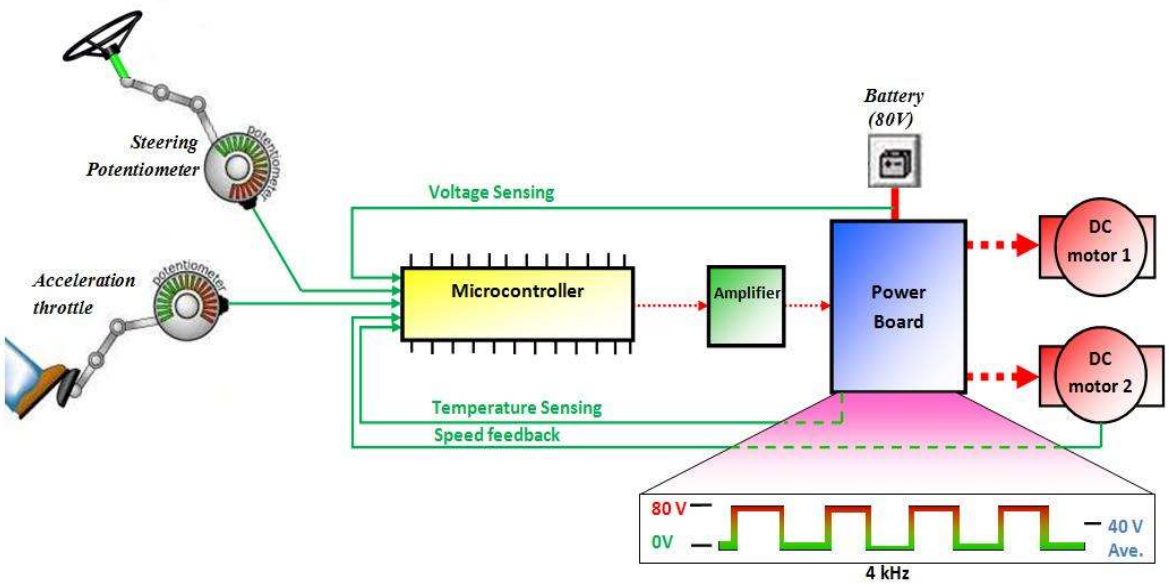

Figure 1. Principle and schematic diagram of designed controller

The Proteus 6 professional software was used to simulate the circuit (Fig. (2)). The circuit consists of 2 IGBT Module (Insulated Gate Bipolar Transistor) (1200V, 800A), two ICL7667 MOSFET/IGBT drivers, one ATmega32 microcontroller with four PWM output ports, one 4×20 digital LCD, one LM35 temperature sensor, one acceleration potentiometer activated by throttle and one steering double potentiometer, two 5 VDC encoder on motor shaft, two 300 A fast diode and other industrial electric and electronic devices such as capacitors, resistances, buttons and fuses. The circuit uses three different voltages; 5V for microcontroller, 12V for IGBT driver and 80V for motors. The CodeVision software was used to write a program in C language and programming microcontroller to communicate between hardware and software. The designed system specifications and capabilities are as follows:

- *Infinitely continuous variation and smooth drive control system*
- *Preventing sudden acceleration by applying High Pedal Disable (HPD) function.*
- *Providing thermal protection circuit.*
- *Under voltage cutback function to protect the system against low battery voltage.*
- *Forward/backward speed selection, using a power switch.*
- *A master key switch, to turn the system off when not in use.*
- *Two power fuses, to protect from accidental shorts.*
- *A two way potentiometer for steering in both ways.*

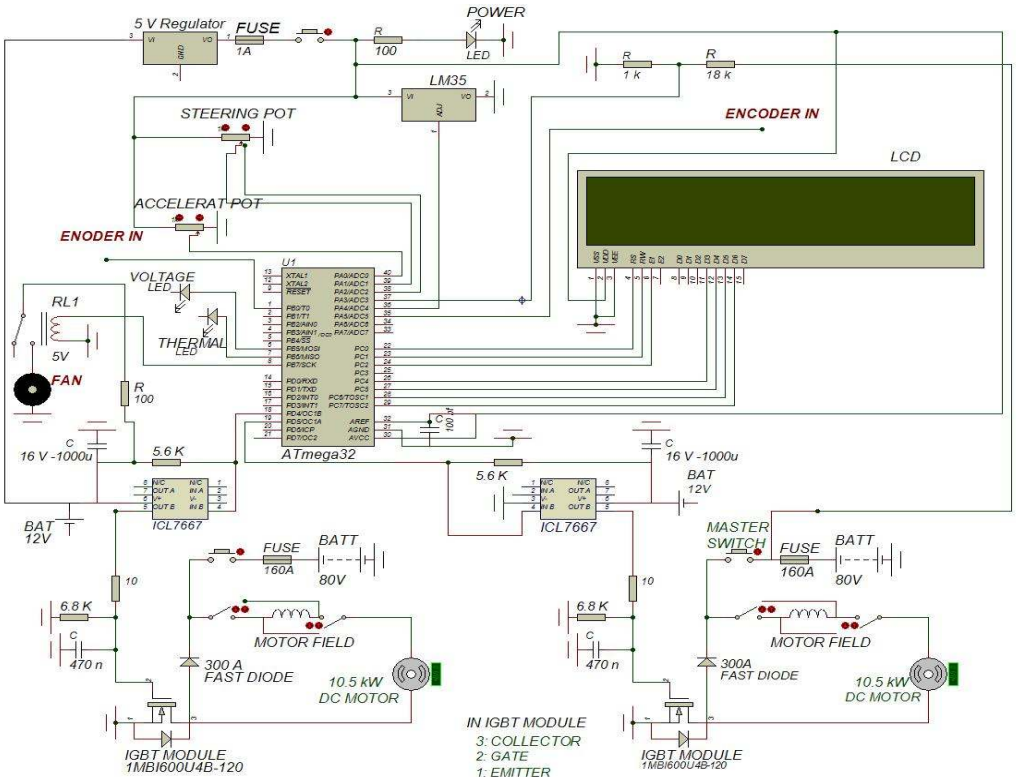

Figure 2. Schematic diagram of the driver designed by Proteus software®.

The amplified PWM voltage from microcontroller is fed to the IGBT gate and control the IGBT. Increasing the IGBT gate voltage enhances the channel of the IGBT and allows more current flow from Collector to the Emitter.

An analogue temperature sensor (LM35) measures the box temperature and cut off the circuit in high temperatures. For low voltages also when voltage of the battery pack falls under unfavorable level, first a LED alarm lights up then the circuit cuts off. HPD function prevents for sudden acceleration, which allows motors to reach their rated speed from stand still in almost 10 seconds.

2.1. Speed-Torque/power characteristics

For an effective design, it is necessary to understand the D.C. motor characteristic curves since for each motor there is a specific Torque-Speed curves. The electric circuit of the armature and the free body diagram of the DC series motor are shown in the Fig. 3.

The KVL equation for this motor is give by [11];

$$V_T = E_A + I_A \,.\, (R_A + R_S) \qquad (1)$$

In a series motor the flux per pole depends upon the armature current and, hence, upon the load, then $\varphi = c.I_A$ (where c is the coefficient between flux and armature current). The conducted torque in this machine is estimated by Eq. (2):

$$T_{ind} = K \,.\, \varphi \,.\, I_A = K \,.\, c.I_A^2 \qquad (2)$$

Where; $K = \frac{Z.p}{2\pi.a}$ so rewriting Eq. (2) in order to I_A, the internal generated voltage as; $E_A = K \,.\, \varphi \,.\, \dot{\theta}$ and Substituting in Eq. (1) leads to:

$$V_T = K \,.\, \varphi \,.\, \dot{\theta} + \sqrt{\frac{T_{ind}}{K \,.c}}\ (R_A + R_S) \qquad (3)$$

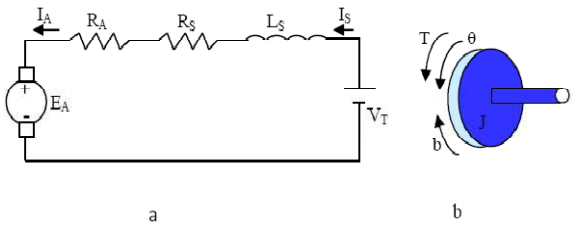

Fig. 3. a) Schematic diagram of a series motor, b) kinematic analyses of motor's rotor

Rewriting $\varphi = c.I_A$ *and Eq. 2 as;* $\varphi = \sqrt{\frac{c}{K}} \cdot \sqrt{T_{ind}}$ *and substituting into Eq. (3) give:*

$$\dot{\theta} = \frac{V_T}{\sqrt{K.c}} \cdot \frac{1}{\sqrt{T_{ind}}} - \frac{R_A + R_S}{K.c} \qquad (4)$$

T_{ind} is defined as a function of N using the following equation:

$$T_{ind} = \frac{E_A . I_A}{\frac{2\pi N}{60}} \qquad (5)$$

Where E_A is defined by Eq. (1), N is derived using the equation; $\frac{E_A}{E_{Ao}} = \frac{N}{N0}$. *Some of the evaluated motor parameters in relation to Speed-Torque characteristics, defined in the Table (1).*

Table 1. DC series motor characteristics

Terminal voltage, V_T	*80 V*
Armature and field resistance, R	*0.085 ohms*
Rated speed, N_0	*2260 rpm*
Rated power, P	*10.5 kW*
Motor constant, K.c	*1.73 * 10^{-3}*
The electromotive force constant, k	*0.277 Nm/Amp*
Moment of inertia of the rotor, J	*1 kg.m^2/s^2*
Mechanical system damping ratio, b	*1 Nms*
Electric inductance, L	*2 H at 4 kHz*

2.2. Control strategy

PWM is critical to modern digital motor controls. By adjusting the pulse width, the speed of motor can be efficiently controlled without many losses. PWM sends a square wave at a certain frequency (4 kHz in this case) to control the IGBT.

Since the transient response of a practical control system often exhibits damped oscillations before reaching steady state, it is desired to position the motor very precisely, thus the steady-state error of the motor position should be zero. Also, the steady-state error due to a disturbance should be zero as well. The other performance requirement is that the motor reaches its final position very quickly (low settling time). In this case it is assumed to have a settling time of 2 second (ts: is the time required for the response curve to reach and stay within a range about the final value, usually 2% or 5% of the final value) and also an overshoot smaller than 10%. The reference input was simulated by a unit step input. If the response to a step input is known, it is mathematically possible to compute the response to any input. Fig. (4) illustrates the schematic diagram of a PID control. The error term, e(t) is derived by subtracting the feedback (motor speed), u(t) from the set point (set speed from input), r(t) as shown in Eq. (6).

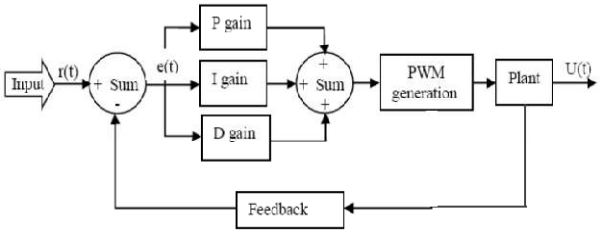

Fig. 4. DC motor control system block diagram

The error is in terms of a number of encoder counts per unit time. For P Gain a simple proportional coefficient K_p is multiplied by the error term. The integral coefficient K_i is multiplied by the error term and added to the sum of all previous integral terms; it provides response to accumulated error. Finally, the derivative coefficient K_d is multiplied by the difference between the previous error and the current error and responds to change in error from one PID cycle to the next. PID control strategy is shown in Eq. (7);

$$e(t) = \text{set speed} - \text{encoder count} = r(t) - u(t) \qquad (6)$$

$$u(t) = K_p . e(t) + \frac{K_i}{T_i} \int_0^t e(t)dt + K_d . T_d \frac{de(t)}{dt} \qquad (7)$$

Where T_i is integral time and T_d is derivative time.

Applying Newton's law in Fig. (3-b), and Kirchhoff's laws in Fig. (3-a) yields Eq. (8) and (9) respectively.

$$J\ddot{\theta} + b\dot{\theta} = (k.\emptyset).I_A \qquad (8)$$

$$L\frac{dI_A}{d_t} + R.I_A = V_T - (K.\emptyset).\dot{\theta} \qquad (9)$$

In Eq. (8), k.φ is the armature constant and in Eq. (9), K.φ is the motor constant (in SI units they are

equal). Using Laplace transform functions from Eqs. 14 and 15, we have:

(Note that: $L\left[\frac{d^2}{dt^2}f(t)\right] = s^2 f(s) - sf(0) - (\dot{f}(0))$*)*

$$J s^2 \theta(s) + b\,\theta(s) = k.I_A(s) \qquad (10)$$
$$(Ls + R).\ I_A(s) = V_T - k.s.\theta(s) \qquad (11)$$

By eliminating $I_A(s)$, the rotor position can be found as a function of terminal voltage (Eq. (12)). For convenience in comparing transient response of various systems, it is a common practice to use the standard initial condition that the system is initially at rest with the output and all time derivatives equal to zero;

$$\frac{\theta}{V_T} = \frac{k}{s\,((J.s+b)(L.s+R)+k^2)} = \frac{k}{(L.J)s^3+(L.b+R.J)s^2+(R.b+k^2)s} \qquad (12)$$

Also the rotational speed $\dot{\theta}$can be derived as a function of terminal voltage:

$$\frac{\dot{\theta}}{V_T} = \frac{k}{(J.s+b)(L.s+R)+k^2} = \frac{k}{(J.L)s^2+(J.R+L.b)s+(b.R+k^2)} \qquad (13)$$

If the motor position (θ), motor speed ($\dot{\theta}$), and armature current (I_A) are chosen as state variables, the state-space representation of these equations can be rewritten as:

$$\frac{d}{dt}\begin{bmatrix}\theta\\ \dot{\theta}\\ I_A\end{bmatrix} = \begin{bmatrix}0 & 1 & 0\\ 0 & -\frac{b}{J} & \frac{k}{J}\\ 0 & -\frac{k}{L} & -\frac{R}{L}\end{bmatrix}\begin{bmatrix}\theta\\ \dot{\theta}\\ I_A\end{bmatrix} + \begin{bmatrix}0\\ 0\\ \frac{1}{L}\end{bmatrix}.V$$

$$Y = [1 \quad 0 \quad 0]\begin{bmatrix}\theta\\ \dot{\theta}\\ I_A\end{bmatrix} \qquad (14)$$

The input is source voltage, V_T and the output is the speed of shaft, $\dot{\theta}$. The rotor and shaft are assumed to be rigid. After replacing the parameters that were given in table (1) into Eq. (13) it can be rewritten as Eq. (15). It can be easily proved that in every closed loop system, by a gain of feedback equal to 1, it tends to equalize the output by input [12].

$$G(s) = \frac{\dot{\theta}}{V_T} = \frac{1}{(s+0.96)(7.22s+0.613)} \qquad (15)$$

3. Results

Equations (1-5) were programmed in MATLAB programming toolbox for different I_A from 10A to 1000A.

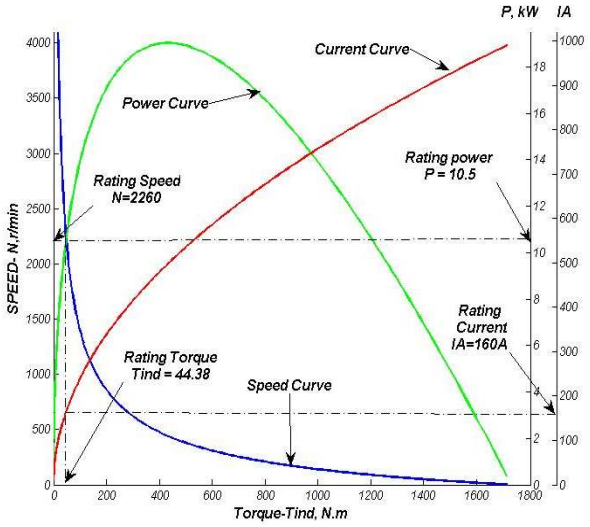

Fig. 5. The speed-torque, current-torque and power- torque diagram for DC series motor

The variation of N and resulted T_{ind}, the rating speed, current and power also is shown as a function of the rating torque in Fig. (5). This figure shows that the torque is inversely proportional to the speed of the output shaft and for start up points the torque and consequently the high power is available. Obviously, if the load is small, the speed may rise to a dangerously high value. Because of providing very high start-up torque, in the start-up the armature current is higher than normal. On the other hand, the high current and low efficiency limits the usage of high powers (the peak of the power diagram). According the data from these motors catalogue, motors efficiency in the rated power can be calculated as:

$$\eta = \frac{P_o}{P_i} = \frac{P_o}{E_A\,.\,I_A} = \frac{10500\ W}{80 * 160\ V.A} = 0.82$$

Fig. (6) shows the experimental PWM pulses generated of the controller. In the Fig. (6-A) very ideal microcontroller generated pulses illustrated. Fig. (6-B) shows the 12 V buffer generated pulse that feed to IGBT gate. As it is seen this pulse is not as ideal as the microcontroller generated pulses.

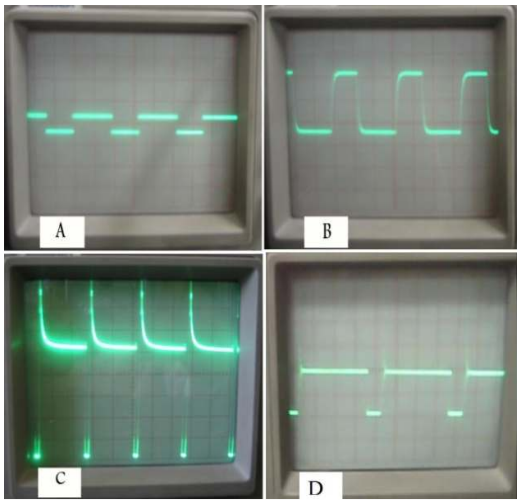

Fig. 6. Oscilloscope illustrated PWM pulse in different steps.

Fig. (6-C) shows the motor switching PWM pulses without fast diode that tracked from collector. Without diode when the IGBT switch to off, a very high surge voltage generated. This surge voltage can cause burning out the controller very fast. To solve this problem a fast diode installed into circuit. The Fig. (6-D) illustrates these pulses after diode. In this case the generated wave is approximately ideal by negligible spike fluctuations in the beginning of cut off.

The system response for distinct P, PI and PID control is evaluated. The simulink model of DC motor by P control is shown in Fig. (7). The system response for different disturbances showed that increasing disturbance, increases the steady-state error value. Typically, the disturbance reaction at four sample disturbances: 5, 10, 15 and 20 values for P control by a constant gain of 10 (K_p =10) and a unit step input is illustrated in Fig. (8). As shown in Fig. (8) increasing the disturbance from 5 to 20 increases the steady state error from around 0.45 to 1.7 for P control.

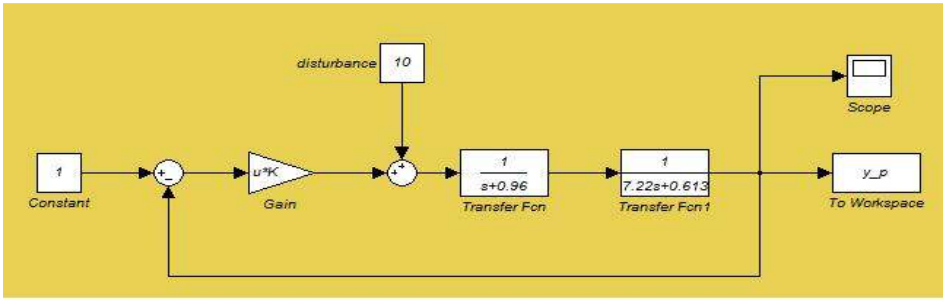

Figure 7. The simulink model of DC motor by P control

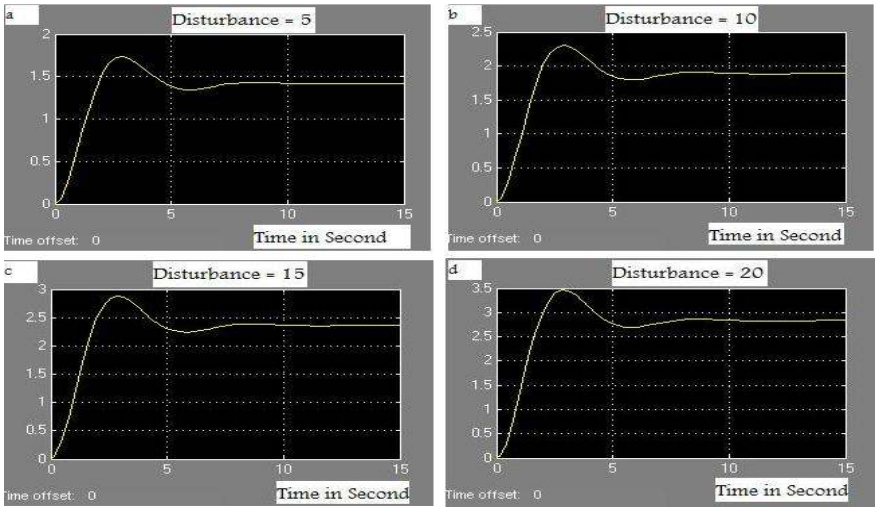

Figure 8. Different disturbance response for P control

The system response for optimum of K_p value evaluated to define the best Kp with minimum steady stat error, overshoot (Maximum overshoot is the maximum peak value of the response curve measured from unity) and settling time. Some of typical results from more than 30 runs are shown in Fig. (9). As illustrated in the figure and according to Eq. (16), increasing K_p value decreases the steady state or offset error and also the overshoot. But its variation has no effect on the settling time. By increasing K_p over to 90, the response also begins to fluctuate. Since none of these cases do not comply with the desired assumptions, the P control is not a good choice to control these motors.

Equation (16) shows the relation between K_p and steady state error [12].

$$e_{ss} = \lim_{t\to\infty} e(t) = \lim_{s\to 0} s.E(s) = \frac{1}{1+K_p} \quad (16)$$

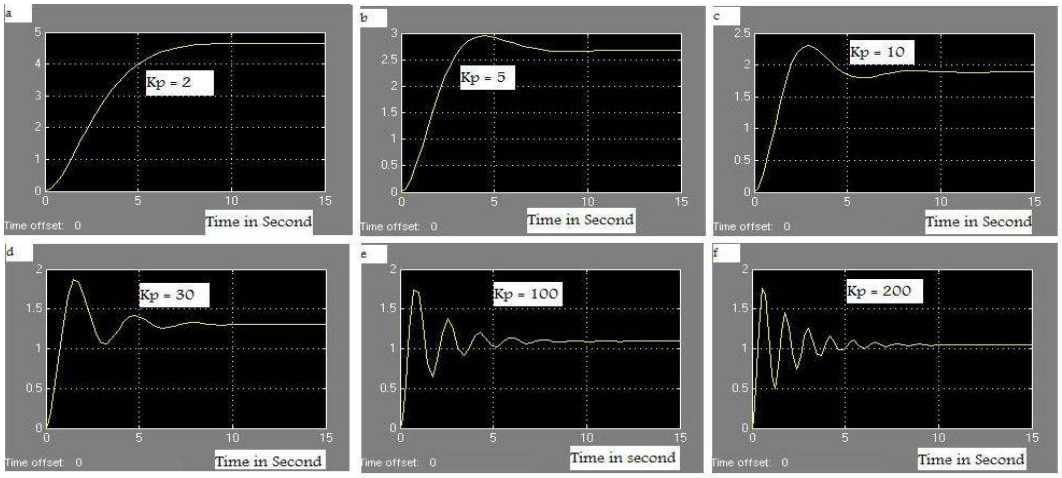

Fig. 9. Different K_p reactions on response at disturbance equal to 10

Using the simulink model the PI control diagram is shown in Fig. (10) that the error term multiplied by both proportional and integral term. A disturbance of 10 was also assumed for this control system. Using the simulink model for PI control, the PI model was tested for different K_p and K_i values. Results showed that for constant K_p, increasing K_i increases the fluctuations until the system output approaches to infinity (Figs 11-d and 11-e). For a constant K_i increasing K_p decrease the overshoot. The plotted diagrams for PI control shows that this system eliminates steady state error. Otherwise in this control system decreasing K_i leads to low settling time and low fluctuations. According to Eq. (17) the integral controller eliminates the offset error [12].

$$e_{ss} = \lim_{t\to\infty} e(t) = \lim_{s\to 0} s.E(s) = 0 \quad (17)$$

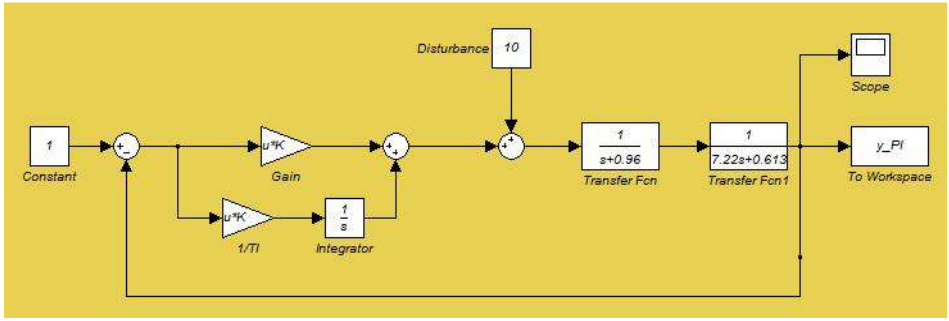

Figure10. Simulink model of PI control for DC motor control

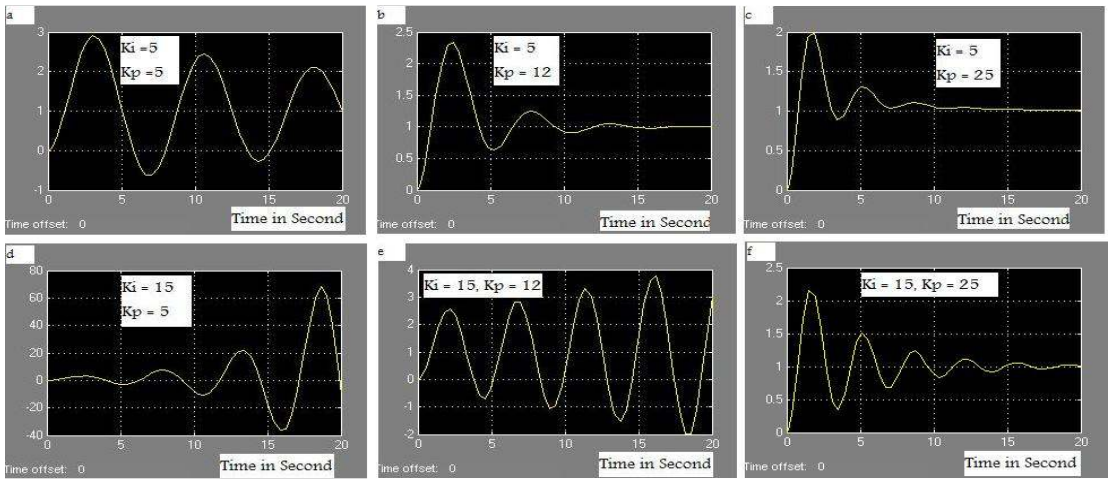

Fig. 11. PI control by different K_i and K_p values

The simulink model of DC motor by PID control is shown in Fig. (12). Many tests were performed for PID control model to obtain best answers for K_p, K_i and K_d. Results showed that for every K_i and K_d, increasing K_p decreases the overshoot. For every K_p and K_d, decreasing K_i, decreases the overshoot and increases the settling time. Fig. (13-i) produces the best response to match the assumptions mentioned earlier. In this mode for K_p= 320, K_i=350 and K_d=40, the overshoot is 0.1(10 % of the full response), the settling time (t_s) is almost 2 s and the overshoot time is smaller than 1 s. Also the peak time is almost 0.5 s, the rise time is almost 0.2 s and the delay time is less than 0.2 s. PID control has the advantages of each of the three individual control actions and it is satisfy the desired assumptions in this research.

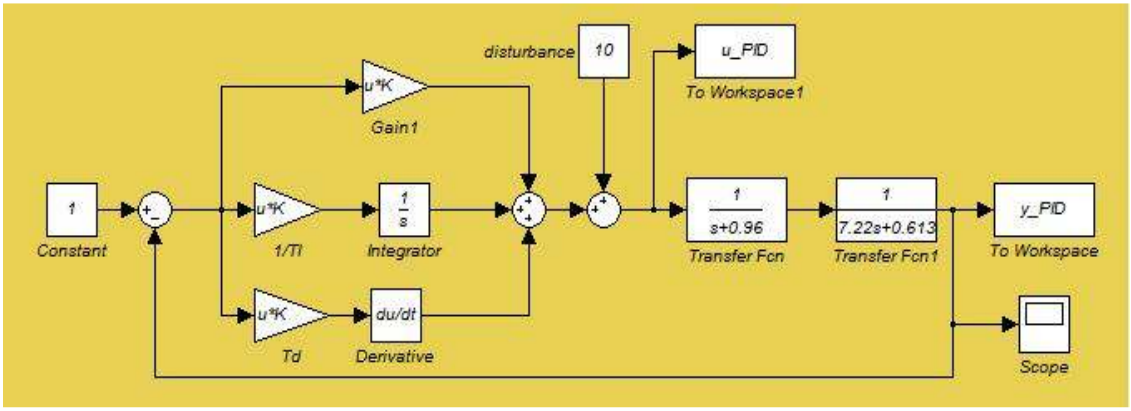

Fig. 12. PID control using simulink model for DC motor

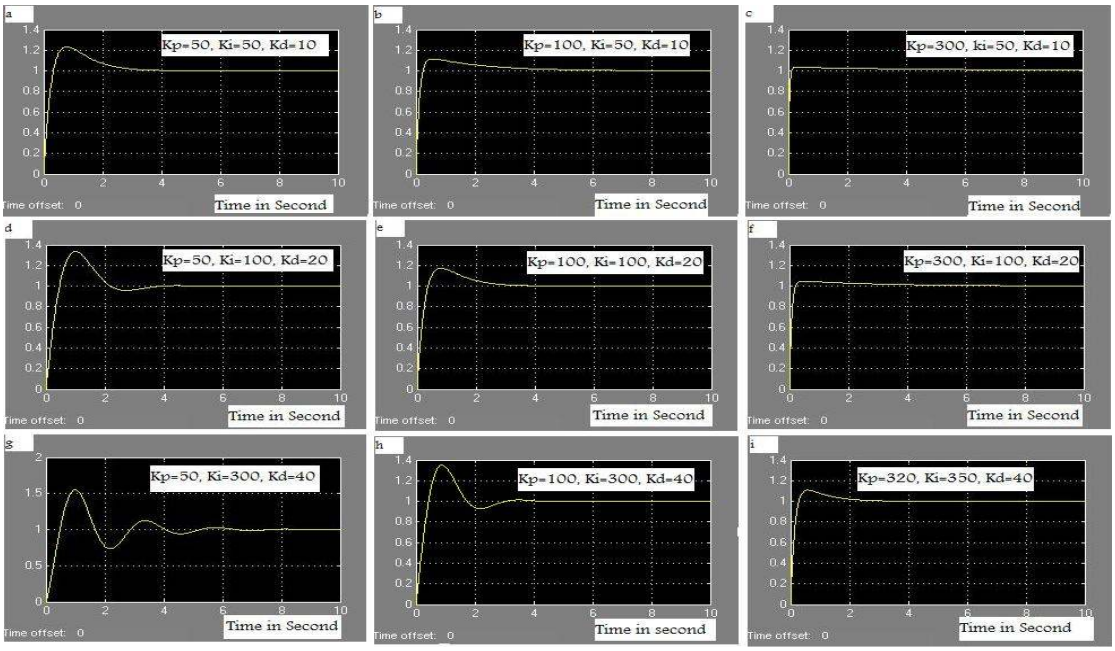

Fig. 13. PID control for different K_p, K_i and K_d values

4. Conclusion

A DC motor driver was designed and constructed to control the speed and direction of two series DC motors. One acceleration pedal, control the speed of both motors simultaneously and differential action between the motors speed activated by steering mechanism. Simulation some characteristics of the selected DC motors in MATLAB programming toolbox, confirmed; in DC series motors high torque is possible at start-up, that make them suitable for traction applications. Also, using MATLAB Simulink the P, PI and PID control strategies were assessed and it was found that the P control creates a steady state error and changing the P control gain coefficient (K_p) is not able to eliminate this error. In PI control mode, although the steady state error is completely eliminated, its overshoot and settling time will not be able to satisfy the aim of the design either. The results for PID control scheme proved to be satisfactory having chosen suitable parameters for K_p, K_i and K_d. From numerous test results, values of 320, 350 and 40 respectively for K_p, K_i and K_d indicated the best response. Those values were selected to be used in the microcontroller programming using CodeVision software. This controller was designed, constructed and evaluated under load condition. The experimental tests gave good results for the controller to be used in any electrical or hybrid vehicles. Although the controller was designed for 30 kW vehicles, by small changes in its program, it can be used for vehicles and electric tractors for up to 100 kW.

References

[1] Silva V, Carvalho V, Vasconcelos R M, Soares F. Remote PID control of a DC motor. Manuscript Paper presented at REV2007 conference, Porto, Portugal, June 2007; iJOE International Journal of Online Engineering: www.i-joe.org.

[2] Mrozek B, Mrozek Z. Modelling and fuzzy control of DC drive. 14-th European simulation multi conference ESM 2000. May 23-26; Ghent: pp186-190.

[3] Pravadalioglu S. Single-chip fuzzy logic controller design and an application on a permanent magnet dc motor. Engineering Applications of Artificial Intelligence 2005; 18: 881–890.

[4] Kumar N S, Sadasivam V, Asan Sukriya H M, Balakrishnan S. Design of low cost universal artificial neuron controller for chopper fed embedded DC drives. Applied Soft Computing 2008; Article in press.

[5] Nouri K, Dhaouadi R, Braiek N B. Adaptive control of a nonlinear dc motor drive using recurrent neural networks. Applied Soft Computing 2008; 8: 371–382.

[6] Thirusakthimurugan P, Dananjayan P. A novel robust speed controller scheme for PMBLDC motor. ISA Transactions 2007; 46: 471–477.

[7] Santana J, Naredo J L, Sandoval F, Grout I, Argueta OJ. Simulation and construction of a speed control for a DC series motor. Mechatronics 2002; 12: 1145–1156.

[8] Massacci C, Usai A, Giamberardino P, D. An embedded approach for motor control boards design in mobile robotics applications. Proceedings of the 10th WSEAS International Conference on Circuits, Vouliagmeni, Athens, Greece, July 10-12, 2006 (pp265-270).

[9] Al-Ayasrah O, Al-Lawama, A. DSP-based two-synchronized motors control system using external FPGA design. WSEAS TRANSACTIONS on SYSTEMS and CONTROL. Issue 4, Volume 3, April 2008(pp279-288).

[10] Xepapas F, Kaletsanos A, Xepapas S, Manias S. Nonlinear Geometric Fuzzy Logic Control for DC Motor Drive Systems. WSEAS International Conference, Rethymno, Greece, July 8-15, 2001.

[11] Stephen J. C. Electric machinery fundamentals. 4th ed. McGraw-Hill Higher Education; 2004.

[12] Ogata, K. Modern control engineering. 4th ed. prentice hall publisher; 2002.